X-ray Astronomy 2000
ASP Conference Series, Vol. in press, 2001
eds. R. Giacconi, L. Stella, S. Serio

Results from the *Chandra* HRC Survey of the Orion Nebula Cluster Region

S. Sciortino, E. Flaccomio, G. Micela, F. Damiani, N. Pizzolato

Osservatorio Astronomico G.S. Vaiana, Palazzo dei Normanni, I-90134 Palermo, Italy

F. R. Harnden, Jr., S. S. Murray, S. J. Wolk

Harvard-Smithsonian Center for Astrophysics, 60 Garden Street, Cambridge, MA 02138

Abstract.
We present results of a 63 ksec *Chandra* HRC-I observation of the Orion Nebula Cluster region. We have detected 742 distinct sources in the surveyed 30'x30' region, one of the most crowded ever studied in the X-ray band-pass. The characteristics of the HRC-I permit the detection of sources whose rates span more than 4 dex in intensity, i.e., Orion members down to $L_X \sim 2.5\ 10^{28}$ erg s^{-1}, 25 times deeper than pre-*Chandra* observations. Most of sources are associated with known Orion Nebula Cluster members. The superb angular resolution of the *Chandra* mirrors essentially eliminates the source confusion problems that have affected all previous X-ray investigations of this region and allows us to explore the relationship between X-ray emission levels and stellar parameters, such as age, mass, rotation rate, etc. Our long uninterrupted observation allows us for the first time to systematically explore variability of a large sample of PMS stars over time scales smaller than $\sim$ 1 day.

1. Introduction

The Great Nebula in Orion (M42, also known as Orion Molecular Cloud - I, OMC-I) at a distance of $\sim$ 440 pc, is the richest and best studied star forming region (SFR) in the Galaxy. While its O- and B-type population has long been known (Warren and Hesser 1977a, 1977b, 1978; Brown et al. 1995), the very richness of the region makes it a difficult target of study, and only recently has its late-type PMS population been systematically surveyed and studied in the optical and near-IR (Hillenbrand 1997; Hillenbrand et al. 1998; Simon et al. 1999) deriving, for the central region, a stellar density of $\sim 2\ 10^4$ stars/pc^3 (Hillenbrand and Hartmann 1998). In a region of 5'x5' around the central θ Orionis O star, Hillenbrand and Carpenter (2000) have obtained infrared photometry in the H and K bands down to K=17.5 mag. At the Orion Nebula Cluster (ONC) distance, this should allow the detection of a brown dwarf of 0.02 $M_\odot$ seen through an A_V of 15 mag. Disks, microjets and the so-called proplyds (i.e., gaseous shells with a distinct comet-like appearance due to strong

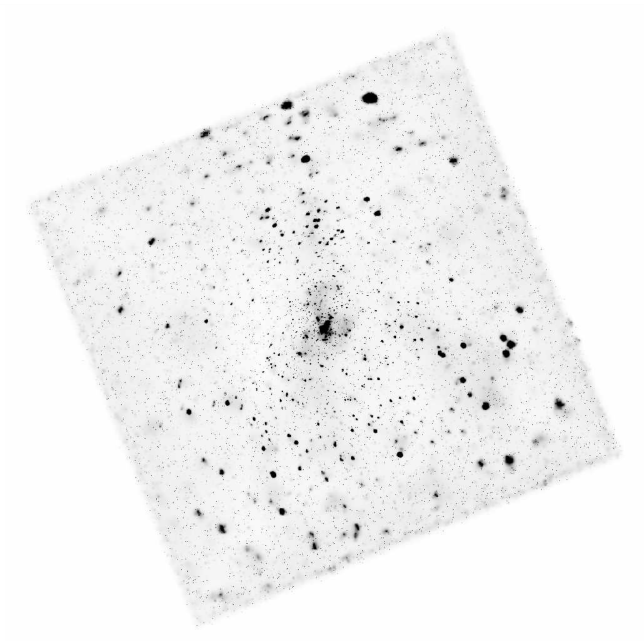

Figure 1. *Chandra* HRC image of the Orion Nebula Cluster region. Data have been smoothed with the adaptive smoothing tool (csmooth) available within CIAO (the Chandra analysis software package - http://chandra.harvard.edu)

.

UV ionizing emission from the central O star inducing disk evaporation) have been the subject of studies based on HST/WFPC2 narrow band images (Bally et al. 2000). An extensive search for disks and candidate protostars has been pursued with JHK and L band surveys (Lada et al. 2000), while extensive campaigns of rotational measurements (Herbst et al. 2000, Stassun et al. 2000) have greatly enlarged the sample of late-type members for which we have rotational data. Studies have been particularly difficult in the X-ray region where angular resolution had been severely limited (cf. Gagné and Caillault 1994, Gagné et al. 1995) until the advent of the *Chandra* X-ray Observatory. For the first time, the deep imaging capabilities of *Chandra* make it possible to explore the X-ray emission at resolutions comparable to that previously available only in other wavelengths.

Garmire et al. (2000) have reported first results from a $\sim$ 48 ksec *Chandra* Advanced CCD Imaging Spectrometer (ACIS; Townsley et al. 2000) image of the central Trapezium region. Here we present results of our ongoing analysis of the first Orion image (cf. Figure 1) obtained with the *Chandra* High Resolution Camera (HRC; Murray et al. 2000) as part of the GTO program.

2. The Data and Source Detection

The ONC was observed continuously for 63 ksec with the HRC-I starting on 2000 February 4 at 19:30. Source analysis using a wavelet-based source detec-

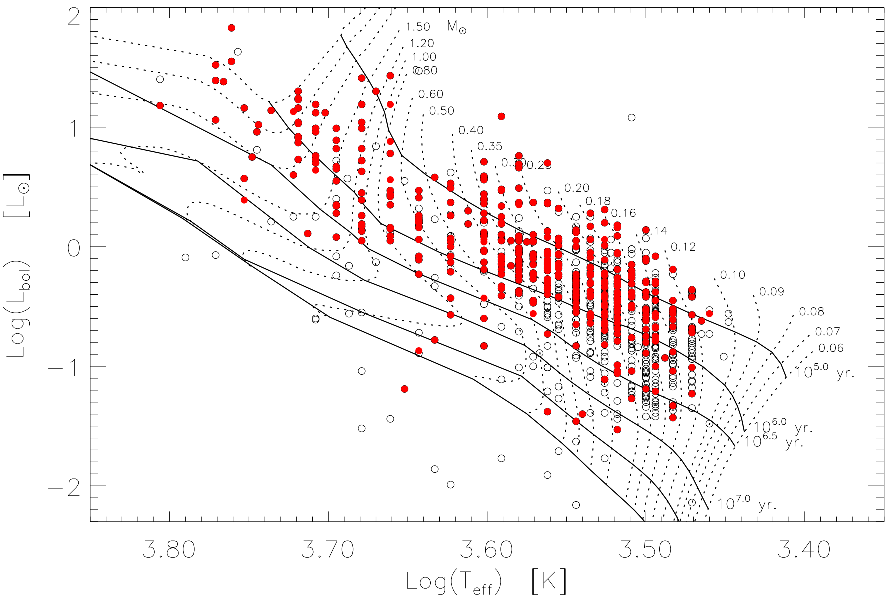

Figure 2. The Luminosity-Temperature diagram for the Orion Nebula Cluster based on the optical sample by Hillenbrand (1997), but for the stars with proper motion membership probability (Jones and Walker 1988) greater than 50%, or unknown. Solid symbols mark the HRC-I detected stars in the above sample. Mass tracks are from D'Antona and Mazzitelli (1997).

tion algorithm, *pwdetect*, developed at the Osservatorio Astronomico di Palermo (Damiani et al. in preparation) has yielded 742 detections from the HRC-I data. Running an extensive set of simulated, pure background HRC-I image we have computed for the actual image background level the expected number of spurious sources as a function of source acceptance threshold. We have chosen a source acceptance threshold for which we expect 10 spurious sources (out of 742) since adopting the more conservative level of 1 spurious source we would have loose $\sim$ 80 sources. Thanks to the very good linearity of the HRC-I, we have detected sources with rates ranging from about 10^{-4} to 2 cnt sec^{-1}, spanning a more than 4 dex range (i.e. over a dynamic range that is currently matched only by VLA observations).

In order to find counterparts of detected sources we have created a master catalog by uniquely joining positions and other available information from several proper motion, optical and near-IR surveys of the region we have observed. Source counterparts have been found by positional matching X-ray and catalogued source positions taking into account uncertainties both on X-ray and other catalog positions. We have found unique counterpart for 693 sources, with a number of sources in the central region having proplyds as counterparts. For about 30 sources we have not found catalogued counterparts, about 10 of these are in the central part of the FOV subject to deep scrutiny in the K band. For the remaining handful of sources, in the external part of

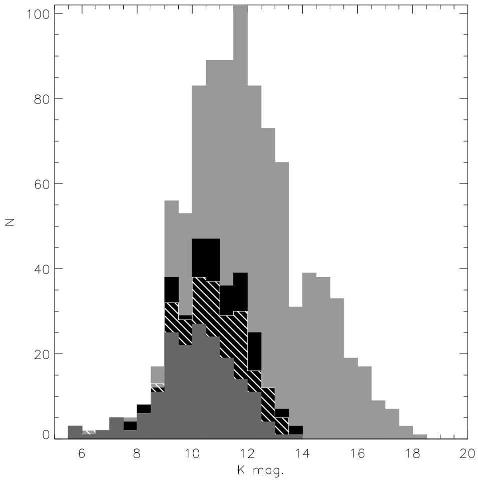

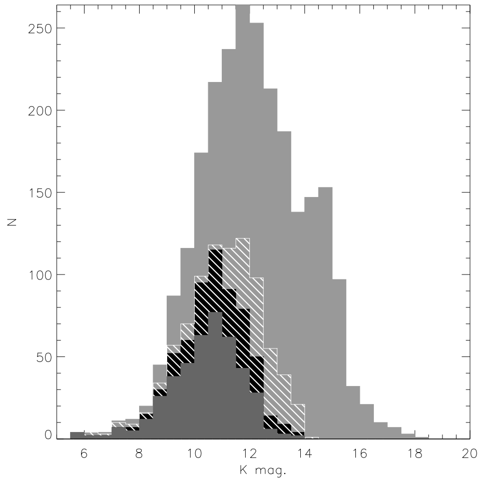

Figure 3. [right] Histograms of number versus magnitude in the K band for the central 4' radius region where deep K band data are available: parent sample (outer gray), detected sample (black), parent sample of stars with known mass and age (hatched gray), sample of detected stars with known mass and age (inner gray). [left] As in the right panel, but extended over the entire HRC-I FOV. Note the clear lack of identified detections for K > 14.

FOV, we have found more than a single counterpart. Indeed the superb angular resolution of the *Chandra* mirrors has eliminated essentially all the source confusion/identification problems affecting previous observations. A visual impression of the effectiveness of the *Chandra* angular resolution can be gained inspecting the figures of the HRC-I observation at increasing zoom presented by Harnden et al. (2000).

For all stars in our master reference catalogue (containing about 2800 stars) that have not been detected we have computed upper-limits to their X-ray emission.

Conversion factors from rate to emitted flux have been computed assuming a single-temperature Raymond-Smith emission model with kT=0.86 keV and N_H derived from the known A_V values of stellar counterparts. A median value of N_H has been assumed for those sources without known A_V. The X-ray luminosities have been computed adopting a distance of 440 pc. Thanks to the very good linear response of the HRC-I we have been able to measure L_X spanning the 2.3 10^{28}–1.2 10^{33} erg/sec range. We have reached a limiting sensitivity 25 better than obtained with previous ROSAT HRI observations and quite similar to that obtained with ACIS-I (Garmire et al. 2000; Hillenbrand and Carpenter, 2000).

A comparison of our source list with the 973 detections reported by Garmire et al. (2000) indicates that even in the central part of the field-of-view a fraction of HRC sources do not correspond to objects seen in the ACIS-I data, in spite of the fact that the ACIS-I observation reached a slightly deeper sensitivity. This implies intense variability of X-ray emission from ONC members.

3. Variability

The continuous 63 ksec HRC-I observation allows us to explore variability on time scale from half an hour to a day. In order to gain a visual perception of the variability we have created a movie from a sequence of 16 consecutive Orion images, each spanning 7.5 ksec and separated by 3.7 ksec. This movie, available on the CD-Rom accompanying this volume in the file /orion/orion_moview.wav) shows that variability is a common phenomenon. In order to more rigorously quantify the occurrence of variability we have systematically analyzed with a Kolmogorov-Smirnov test the distribution of photon arrival times for all sources and have considered the three groups of sources for which we can reject the null-hypothesis that the emission is compatible with a constant source at the 90%, 95% and 99% confidence levels. These three groups are populated by 243, 200 and 134 sources, respectively. A graphical summary of our analysis for the sources in the central part of the surveyed region is shown in Figure 4, while in Figure 5 we summarize the result of our variability analysis as a function of X-ray luminosity and L_X/L_{Bol}. Note that as the intensity of source increases we detect more and more variable sources, while given the size of error bars it is unclear whether or not variability is more common for sources near the saturation limit (e.g., $\log L_X/L_{Bol} \sim -3.0$).

In Figure 6 we show examples of the available data for two variable sources. The upper part of Figure 6 summarizes the data for a M1 PMS star. This star has been detected only because of a strong flare followed by a sustained increase of "quiescent" X-ray emission level. The second source, detected only because of the occurrence of a strong flare, has no catalogued counterpart down to K $\sim$ 17.5. There is no suggestion of any emission at its position in the 2-MASS K-band image.

4. Nature of the unidentified sources

About 10 unidentified sources fall in the central region of the FOV that has been scrutinized in the K band down to 17.5 mag. An example of such a source is shown in the bottom part of Figure 6. It is worth to note that Lada et al. (2000) have performed a deep L band study of the region around this source and have indeed found two protostar candidates in its vicinity, but none coincides with the position of this X-ray source. We argue that the likely counterparts of such an unidentified source (as well as of the others mentioned above) belong to two possible classes: very low-mass stars/brown-dwarfs or strongly absorbed near Class-0 PMS stars.

5. X-ray vs. other stellar parameters

Taking advantage of our determination of X-ray luminosity, L_X, and of the bolometric luminosity, L_{Bol}, computed by Hillenbrand (1997) we have searched for possible relations among L_X and $\mathrm{L}_X/\mathrm{L}_{Bol}$ and other stellar parameters such as mass, age, rotational period, etc. While our analysis is still in progress some patterns are clearly evident in the data as shown in Figure 7. L_X increases with L_{Bol} over a relatively large range of mass and a relation is particularly evident

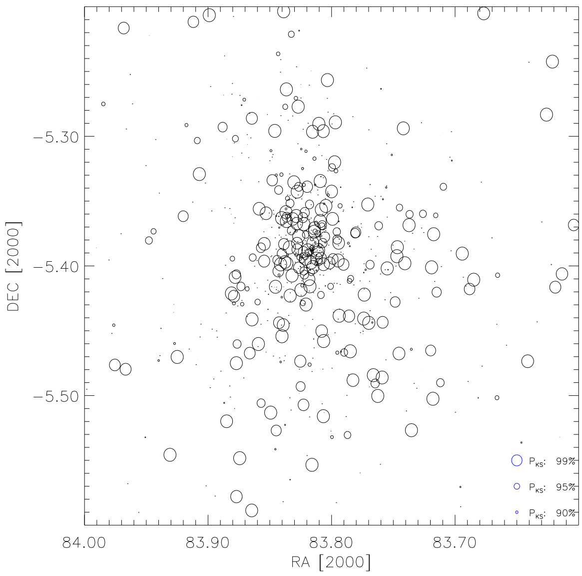

Figure 4. Variability bubblegram for sources in the central part of the FOV. Bubble radius measures the probability at which we can reject the hypothesis that a given source is compatible with being constant. The bubbles on the lower-right show the absolute scale of attained probability.

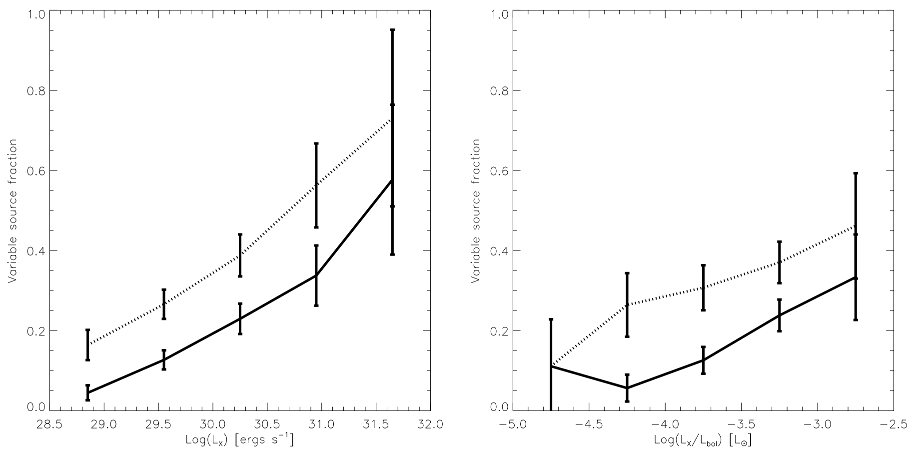

Figure 5. [Right] Fraction of sources found to be variable at KS-test probabilities of 90 and 99 % (dotted and solid lines, respectively), as a function of log L_X.. [Left] Same as on right panel, but for log L_X/L_{Bol}.

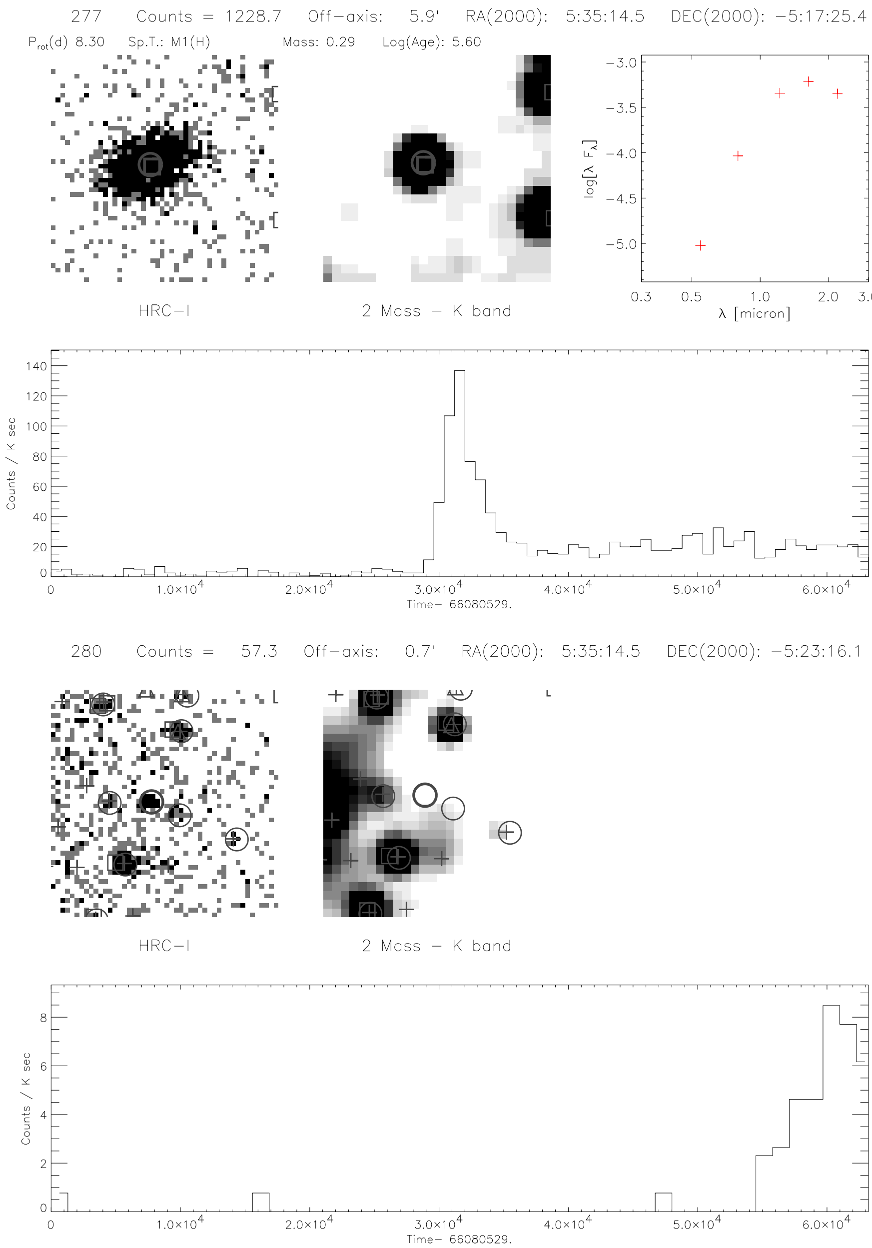

Figure 6. Examples of available data and light-curves for two variable sources (4 plots for each source). [Upper-left panel] HRC 25" × 25" image centered at the X-ray source position; circles indicate X-ray sources, squares stars from Hillenbrand (1997), crosses stars from the deeper Hillenbrand and Carpenter (2000) IR catalog, triangles protostar candidates from Lada et al. (2000). A thick circle marks the source for which we report addtional information and the light curve. [Upper-center panel] 2-MASS K band image (same size of HRC one) centered on the X-ray source position. [Upper-right panel] Optical/Infrared spectrum of the stellar counterpart (blank if no counterpart is found). In the upper two rows are reported: (upper row) a running number, net counts, off-axis (arcmin), RA and Dec of X-ray source; (lower row) rotational period, spectral type, mass (solar mass unit), and log(age) (years) of stellar counterpart. [Lower panel] X-ray source light curve.

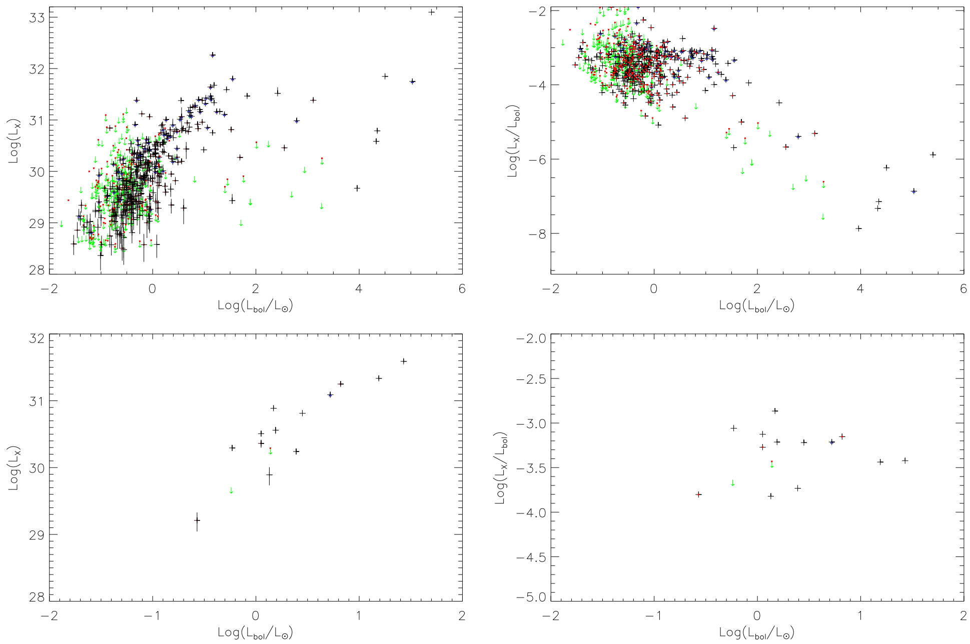

Figure 7. L_X and L_X/L_{Bol} as a function of L_{Bol} for the sample of $\sim$ 700 Orion PMS stars identified as counterparts of X-ray sources. Upper-limits are indicated by arrows. (Upper-left) Log L_X vs. Log L_{Bol} for the entire sample. Note the trend of increasing L_X with L_{Bol}. (Upper-right) Log L_X/L_{Bol} vs. Log L_{Bol} for the entire sample. The large majority of stars have Log L_X/L_{Bol} in the -3 – -4 range (i.e. near the saturation limit), but for the highest luminosity stars, Log L_X/L_{Bol} decreases with increasing L_{Bol}. (Lower-left) As above, but for the stars in the 0.8-1.2 $M_\odot$ range. A clear correlation between Log L_X and Log L_{Bol} is present in the data. (Lower-right) Log L_X/L_{Bol} vs. Log L_{Bol} for the stars in the 0.8-1.2 $M_\odot$ range.

for the case of solar-mass stars. This correlation between L_X and L_{Bol} is likely a byproduct of the late-type ONC PMS stars being saturated. The saturation occurs for log (L_X/L_{Bol}) $\sim$ -3.0, as for normal main-sequence stars. The high-mass ONC PMS stars are far from being saturated, and their (L_X/L_{Bol}) decrease with increasing L_{Bol}. As shown in Figure 8, in the case of the solar-mass stars there is some evidence that log (L_X/L_{Bol}) decreases at higher L_{Bol} for the slow-rotating stars.

6. Summary

With *Chandra's* continuous viewing capability, our $\sim$63 ksec Orion observation permits us to explore variability on time scales from about 30 minutes to a day. With the HRC data, we have detected 742 sources with rates ranging from about 10^{-4} to 2 cnt sec^{-1}, corresponding to log(L_X) spanning nearly four

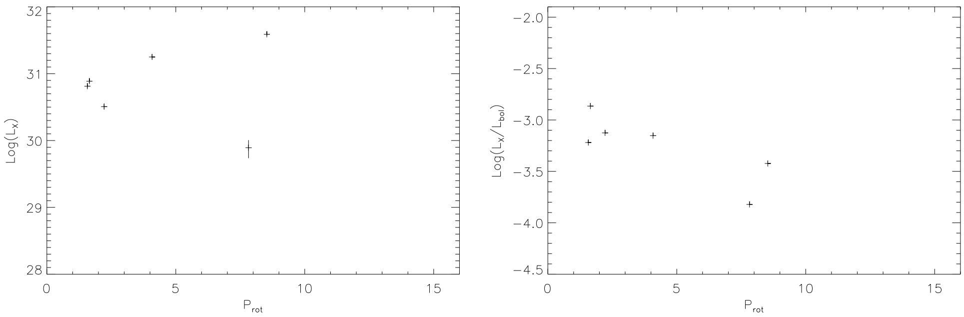

Figure 8. L_X and L_X/L_{Bol} as a function of the rotational period, P_{Rot}, for the sample of PMS stars with mass in the 0.8–1.2 $M_\odot$ range.

orders of magnitude (28.36 to 33.08). We have identified all but about 10 of the sources. Taking advantage of this large sample of PMS stars in ONC, we have found evidence of X-ray emission from proplyds and have found that intense X-ray variability is a common phenomenon which in some cases permits the detection X-ray emission from very faint (brown-dwarf?) or very absorbed (Class-0) PMS stars. Most of the solar-like stars are indeed saturated, and this easily explains the tight relation we have observed between the X-ray and the bolometric luminosity.

Acknowledgments. F.D., E.F., G.M., N.P. and S.S. wish to acknowledge support from Italian Space Agency (ASI) and MURST. Work at the CfA was partially supported by NASA contracts NAS8-39073 and NAS8-38248 and by NASA grant NAS5-4967. E.F. and N.P. acknowledge the hospitality of the CfA.

References

Brown, A. G. A., de Geus, E. J., de Zeeuw, P. T. 1995, A&A, 289, 101

D'Antona F., Mazzitelli, I. 1997, in Cool Stars in Clusters and Associations, eds. G. Micela, R. Pallavicini and S. Sciortino, Mem. SAIt, 68, 807

Garmire, G., Feigelson, E. D., Broos, P., Hillenbrand, L. A., Pravdo, S. H., Townsley, L., Tsuboi, Y. 2000, AJ, 120, 1426

Gagné, M., Caillault, J.-P. 1994, ApJ, 437, 361

Gagné, M., Caillault J.-P., Stauffer, J. R. 1995, ApJ, 445, 313

Harnden, F.R. Jr., Murray, S. S., Wolk, S., Damiani, F., Flaccomio, E., Micela, G., Pizzolato, N., Sciortino, S. 2000, Proceedings of "From Darkness to Light", P. André and T. Montmerle (eds), PASP , in press.

Herbst, W., Rhode, K. L., Hillenbrand, L. A., Curran, G. 2000, ApJ, 119, 261

Hillenbrand, L. A. 1997, AJ, 113, 1733

Hillenbrand, L. A., Hartmann, L. W 1998, ApJ, 429, 540

Hillenbrand, L. A., Carpenter, J. M. 2000, ApJ, 540, 236

Hillenbrand, L. A., Strom, S.E., Calvet, N., Merrill, K. M., Gatley, I., Makidon, R. M., Meyer, M. R., and Skrutskie, M. F. 1998, AJ, 116, 1816

Hillenbrand, L. A., Carpenter, J. M. 2001, Proceedings of "From Darkness to Light", P. André and T. Montmerle (eds), PASP , in press.

Jones, B. F., Walker M. F. 1988, AJ, 95, 1755

Lada, C. J., Muench, A. A., Haish, K E., Jr., Lada, E. A., Alves, J. F., Tollenstrup. E. V., Willner, S. P. 2000, AJ, in press

Murray, S. S., Austin, G., Chappell, J. H., Gomes, J., Kenter, A., Kraft, R., Meehan, G., Zombeck, M., Fraser, G., Serio, S. 2000, SPIE, 4012, 68

Simon, M., Beck, T. L., Greene. T. P., Howell, R. R., Lumsden, S., Prato, L. 1999, AJ, 117, 1594

Stassun, K. G., Mathieu, R. D., Mazeh, T., Vrba, F. J. 1999, AJ, 117, 2941

Townsley, L. K., Broos, P. S., Garmire, G. P., Nousek, J. A. 2000, ApJ Letters, 534, L139

Warren, W. H., Hesser, J. E. 1977a, ApJS, 34, 115

Warren, W. H., Hesser, J. E. 1977b, ApJS, 34, 207

Warren, W. H., Hesser, J. E. 1978, ApJS, 36, 497